Available online at www.sciencedirect.com

ScienceDirect

www.elsevier.com/locate/jes

JES JOURNAL OF ENVIRONMENTAL SCIENCES

www.jesc.ac.cn

Enzymatic preparation of hydrophobic biomass with one-pot synthesis and the oil removal performance

Dan Peng[1], *Wenjie Li*[1,2], *Xujun Liang*[3,4,*], *Liuchun Zheng*[5], *Xuetao Guo*[6,*]

[1] *Department of Transportation and Environment, Shenzhen Institute of Information Technology, Shenzhen 518172, China*
[2] *School of Earth and Environment, Anhui University of Science & Technology, Huainan 232001, China*
[3] *School of Resources and Environmental Science, Quanzhou Normal University, Quanzhou 362000, China*
[4] *Department of Civil and Environmental Engineering, University of Michigan, Ann Arbor, MI 481092125, USA*
[5] *School of Environment, South China Normal University, Guangzhou Higher Education Mega Center, Guangzhou 510006, China*
[6] *College of Natural Resources and Environment, Northwest A&F University, Yangling 712100, China*

ARTICLE INFO

Article history:
Received 29 July 2021
Revised 15 October 2021
Accepted 16 October 2021
Available online 1 February 2022

Keywords:
Biomass
Enzymatic modification
Hydrophobicity
Oil sorption
Two-dimensional correlation spectroscopy

ABSTRACT

Oil pollution is causing deleterious damage to aquatic ecosystems and human health. The utilization of agricultural waste such as corn stalk (CS) to produce biosorbents has been considered an ecofriendly and efficient approach for removing oil. However, most previous studies focused on the modification of the whole CS, which is inefficient due to the heterogeneity of CS. In this study, corn stalk pith (CP), which has excellent amphipathic characteristics, was selected to prepare a high-efficiency oil sorbent by grafting dodecyl gallate (DG, a long-chain alkyl) onto CP surface lignin via laccase mediation. The modified biomass (DGCP) shows high hydrophobicity (water contact angle = 140.2°) and superoleophilicity (oil contact angle = 0°) and exhibits a high oil sorption capacity (46.43 g/g). In addition, DGCP has good stability and reusability for adsorbing oil from the aqueous phase. Kinetic and isotherm models and two-dimensional correlation spectroscopy integrated with FTIR analyses revealed that the main sorption mechanism involves the H-bond effect, hydrophobic effect and van der Waals force. This work provides an ecofriendly method to prepare oil sorbents and new insights into the mechanisms underlying the removal of spilled oil from wastewater.

Introduction

Oil pollution in water bodies causes disastrous damage to the entire ecosystem and results in considerable economic losses to human society. Therefore, a cost-effective and environmentally beneficial technology is required to control oil contamination. Sorption is frequently used to address severe oil water pollution because it is simple to utilize, can be scaled up, is

* Corresponding authors.
E-mails: liangxj@qztc.edu.cn (X. Liang), guoxuetao2005@nwafu.edu.cn (X. Guo).

https://doi.org/10.1016/j.jes.2021.10.019
1001-0742/

inexpensive and is able to recover spilled oil (Oliveira et al., 2021). A series of materials have been used to remove oil from wastewater and oceans, such as synthetic polymers, mineral materials and carbon-based materials, but these materials are nonbiodegradable and, thus, remain in the environment for a long period. The area available for landfills is limited, and further incineration capacities require high capital investment and cause additional environmental damage. These issues have prompted the design and manufacture of ecofriendly materials from renewable sources to replace conventional nonbiodegradable materials. For this reason, it is wise to use biomass, as it is an ecofriendly sorbent, rather than a synthetic material (Zhu et al., 2020). To date, a variety of high-performance oil sorbents have been successfully fabricated based on biomass, including cotton (Zhang et al., 2020), sawdust (Yin et al., 2020), biochar (Navarathna et al., 2020), lignocellulosic fibers (Kang et al., 2020), marine green algae (Xue et al., 2021) and cellulose nanocrystals (Zhang et al., 2019). The wettability of the biomass surface is usually hydrophilic, as there are a large number of hydroxyl groups on the cellulose and hemicellulose of biomass surfaces, providing unsatisfactory results, i.e., poor oil/water selectivity, buoyancy and sorption efficiency. Modifying the surface of the biomass can minimize the hydrophilicity and improve the separation efficiency (Luo et al., 2019). With regard to the functional sites on biomass, a range of chemical reactions, including silylanization, esterification, acetylation, and graft polymerization, have been utilized for surface modification. However, complicated procedures, harsh reaction conditions and toxic chemicals are usually required in these processes.

The material basis of a sustainable society requires changing the nature of the very definition of "performance" from function alone to function and sustainability through thoughtful and green design (Zimmerman et al., 2020). Biomodification methods able to produce high-performance oil sorbents have attracted great attention from both industries and researchers due to their mild and green reaction conditions. Cao et al. (2008) used corn starch to produce porous materials with high oil sorption rates under the combined action of α-amylase and glucoamylase. Our laboratory previously started work in this field by using cellulase and cellulose-degrading fungi (*Aspergillus niger*) and lignin-degrading fungi (white rot fungus) to produce an oil sorbent material (Lan et al., 2013). A deficiency of the previous works was that the hydrophobicity of the biomass was not significantly improved. To improve the hydrophobicity of straw materials, enzymatic esterification, transesterification and grafting of fatty acids and organic esters on the surfaces of straw materials have been reported (Ni et al., 2021). Laccase (EC 1.10.3.2) is a type of polyphenol oxidase that can oxidize a variety of compounds without producing other byproducts and is considered a green biocatalyst. However, due to its low redox potential, mediators with low molecular weight and low redox potential are usually used to increase the laccase substrate affinity, the process of which is called the laccase/medium system (LMS) (Filgueira et al., 2017). The LMS can catalyze and graft hydrophobic chemicals onto lignocellulose to improve its hydrophobicity (Zhou et al., 2020).

Herein, corn stalk pith (CP) was employed to prepare the oil sorbent through a one-pot green method using laccase as a biocatalyst and dodecyl gallate ($C_{19}H_{30}O_5$, DG) as a hydrophobic grafting agent. The main purposes of this work were (1) to explore the surface properties and microstructure of the DG-grafted CP oil sorbent (DGCP, (2) to evaluate the oil sorption capacity of DGCP, and (3) to understand the mechanisms of the DGCP-oil interaction through two-dimensional correlation spectroscopy (2D-COS) integrated with FTIR analyses and several sorption models. The results provide an ecofriendly and efficient method for the preparation of promising oil biosorbents and offer further insight into the mechanism of oil sorption by biomass in aqueous phases.

1. Materials and methods

1.1. Materials and chemicals

CS was harvested in Guangxi Province, China. The pith (CP) was manually peeled from the baled CS, cleaned with water, and then air dried. The CP was first cut into 2-3 cm^3 cubes, ground to the desired particle sizes (20-40 mesh) using a knife mill (Taisite FW135, China), and then placed into hot water for 60 min. After that, the CP was washed with Milli-Q water (Merck Millipore, France) and dried in an oven at 50 °C for 24 hr. The pretreatment samples were stored in a desiccator for future use.

Dodecyl gallate (DG), laccase from *Trametes versicolor* with an activity of 0.99 U/mg, and 2,2′-azino-bis(3-ethylbenzothiazoline-6-sulfonate) (ABTS), all with the highest purity, were acquired from Sigma-Aldrich (USA). The enzyme activity determination information is detailed in the Appendix A Note S1. Guaiacol was supplied by Aladdin (Shanghai, China). The test oil was machine oil with a density of 0.843 g/cm^3 and a viscosity of 14.45 cp at 20 °C (Shell 5w-40). All other chemicals were of analytical grade and used without further purification.

1.2. Preparation of hydrophobic/oleophilic CP

The DG solution was obtained by mixing a certain quantity of DG with 10 mL of ethanol and ultrasonicating the resulting mixture to yield a uniform suspension. This stock solution was used for the formation of hydrophobic/oleophilic CP.

The pretreatment CP (1 g) was immersed in 60 mL of sodium acetate buffer (50 mmol/L, pH 4.8) with laccase (100 U/g), placed in a shaking bath at 45 °C and then continuously stirred for 1 hr under an air atmosphere at 150 rpm. To reach hydrophobicity, the sample was additionally modified by drop casting 10 mL of DG solution (0.25 mmol) and guaiacol (0.25 mmol/L) for 6 hr, followed by subsequent heating in an oven at 105 °C for 1 hr. Upon completion, the obtained product was collected by filtration, followed by a two-step ultrasonic cleaning process using ethanol and distilled water to remove the unbound DG. The washed product was dried in an oven at 50 °C for 24 hr and is referred to hereinafter as DGCP.

The following three different controls were also used in parallel: control 1 (a buffer control without the addition of DG and laccase), control 2 (a laccase control without the addition of DG), and control 3 (a DG control without the addition of laccase).

1.3. Characterization

The surface morphologies of both raw CP and modified CP (DGCP) were observed by scanning electron microscopy, Gemini SEM 300 (SEM, ZEISS, Germany). The surface areas and pore sizes were obtained using the nitrogen adsorption technique at −195.86 °C with a Brunauer-Emmett-Teller analyzer, ASAP 2020 (BET, Micromeritics, USA). X-ray photoelectron spectroscopy, ESCALAB XI+ (XPS, Thermo Fisher Scientific, UK) was used to identify the quantitative elemental and chemical states and the functional groups on all materials. The crystal structures of the as-prepared materials were analyzed using X-ray diffraction (XRD, BRUKER, Germany). The scanning diffraction angle was set to vary from 5° to 60° at a speed of 2°/min and with a step size of 0.02°. The crystallinity index (CrI) is a parameter commonly used to quantify the proportion of crystallization area in cellulosic materials and was determined by the following equation:

$$CrI(\%) = \frac{(I_{21.8} - I_{15.8})}{I_{21.8}} \times 100\% \quad (1)$$

The elemental compositions of all samples (C, H and N) were analyzed via an elemental analyzer (Elementar, Germany), while the O content was calculated by the mass difference, and the (O + N)/C atomic ratio was used to assess the polarity of the materials.

1.4. Surface property analysis

A dynamic contact angle analyzer (OCA15EC, Data physics, Germany) was used to measure the water contact angle (WCA) and oil contact angle (OCA) on the surface of the CP and those on the surface of the DGCP to evaluate the hydrophobicity. The volume of ultrapure water or the volume of oil droplets was 5 μL, and images of the liquid droplets were recorded by DROP imaging. The average values of the WCA and OCA were determined by the circle fitting method at five different locations on the same sample.

The surface energies of the samples were determined based on the Owens–Wendt–Rabel–Kaelble (OWRK) method (Owens and Went, 1969); more information is detailed in the Appendix A Note S2.

1.5. Stability measurements

The corrosion stability of DGCP was evaluated through the following process: the sample was immersed in solutions with varying pH and salt concentrations for 6 hr, rinsed with alcohol and then dried in an oven at 60 °C for 24 hr. Then, WCA and OCA measurements were performed.

1.6. Oil sorption capacity

All sorption experiments were performed following the procedure adopted in our previous work. A modification was utilized in the sorption bag, which was made of a nylon material with a 120 μm pore size. The bag was weighed, and approximately 0.05 g (m_s) of sorbent was placed into the bag. All the bags were then suspended in a certain amount of liquid (150 mL of deionized water and a designated quantity of oil). After a certain time, the bag was lifted, and the excess oil was removed by gently dabbing the bottom of the bag. Then, the final weight of the oil sorbent (m_{so}) was recorded. The following equation was used to estimate the sorption capacity:

$$q = \frac{m_{so} - m_s}{m_s} \quad (2)$$

Duplicate sets were set up in all the experimental studies, and the average values were reported. The details of the sorption kinetics and sorption isotherm models are presented in the Appendix A Note S3 and S4.

1.7. FT-IR and 2D-COS analysis

Fourier transform infrared spectroscopy, Vetex70 (FT-IR, Bruker, Germany), was carried out to analyze the compositions and functional groups of the material. A two-dimensional correlation spectroscopy (2D-COS) analysis using 2Dshige software (Shigeaki Morita, Japan) is detailed in the Appendix A Note S5.

2. Results and discussion

2.1. Surface properties of the DGCP

The WCA and OCA were measured to assess the hydrophobicity and oleophilicity of the LMS-modified CP. The higher the WCA is, the higher the hydrophobicity of modified CP (Zhang et al., 2020). The surface wettability of the sample may be controlled by the conditions of the grafting reaction between DG and CP. As shown in Fig. 1a, the WCAs of samples prepared at different modification temperatures were always higher than 100°, and all exhibited hydrophobicity. The WCA value reached a maximum of 120.5° when the modification temperature reached 45 °C, and the OCA was as low as 38.5°. Modification temperatures below this level or those continuing to increase are not conducive to the hydrophobic and lipophilic properties of the product. This result can be attributed to the wide optimal temperature range of laccase, which differs from one strain to another (Mogharabi and Faramarzi, 2014). Deviation from this temperature will reduce its activity and affect the catalysis of enzymes.

For the enzymatic hydrophobization of CP, gallate compounds are particularly interesting because their surface hydrophilicity can be adjusted. The amount of DG used for modification plays an important role in the grafting of hydrophobic groups onto lignin-based materials. Therefore, the effect of the DG dosage on the amphiphilicity of the CP was studied, as depicted in Fig. 1b. After the introduction of DG, the WCA of the CP increased, confirming that DG can reduce the surface energy and then improve the hydrophobicity of the material. The best lipophilicity and hydrophobicity were exhibited when the dose of DG was 0.25 mmol/L. When the DG exceeded the optimum dosage, the WCA progressively decreased. This decrease occurred because of the combination of grafts containing a large number of nonpolar groups and the rough microscale surface of the material. The dosage of DG determines the number of nonpolar groups in the product, but the dosage

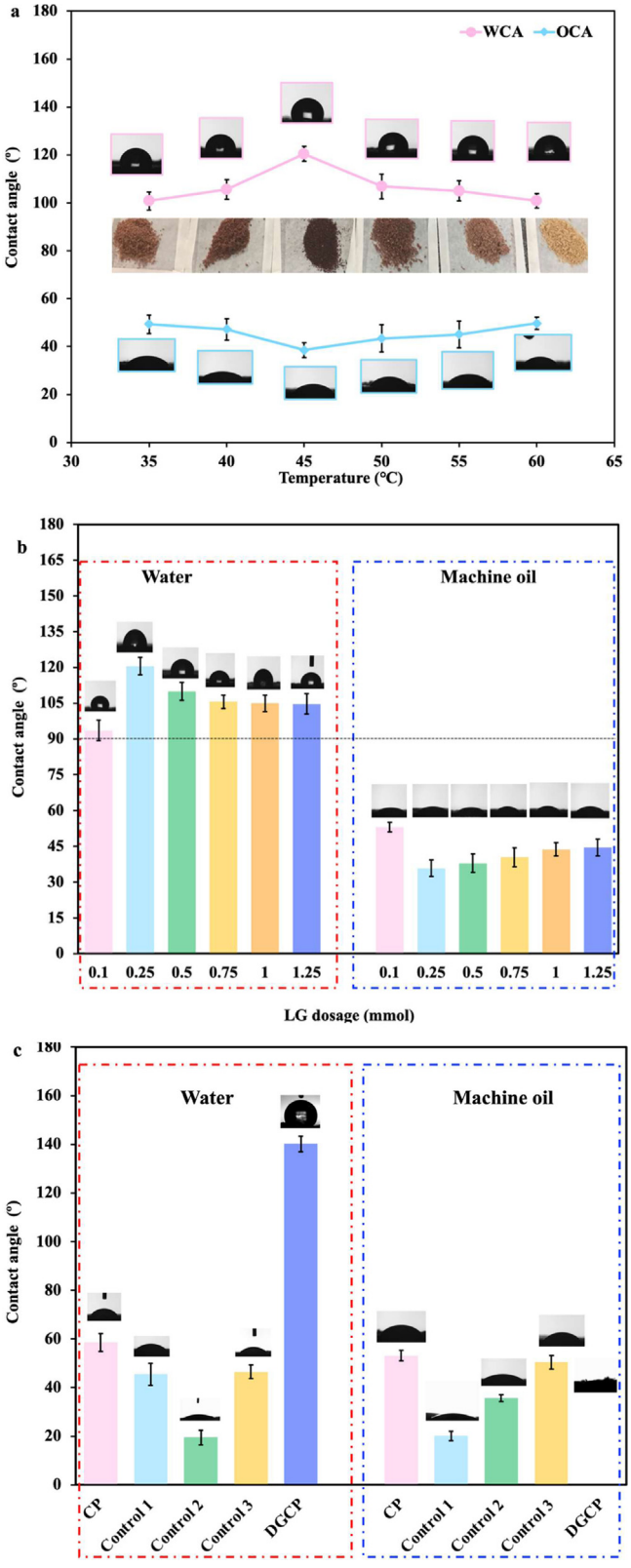

Fig. 1 – The effect of (a) the modification temperature and (b) DG dose on the WCA/OCA of DGCP. (c) Comparison of the WCA/OCA among CP, DGCP and three control conditions. Control 1 (a buffer control without the addition of DG and laccase), control 2 (a laccase control without the addition of DG), and control 3 (a DG control without the addition of laccase).

required for grafts also depends on the number of grafting sites of the material itself. Adding too much DG during the modification process will block the pores of the material and reduce the grafting effect. Thus, adding 0.25 mmol/L DG and reacting at 45 °C is the best condition for preparing hydrophobic/lipophilic DGCP.

The raw CP exhibited hydrophilicity due to the presence of many hydroxyl groups. The WCA and OCA of the CP prepared under the control 1 condition were both reduced slightly (Fig. 1c), which was attributed to the surface lipids and lignocellulose being partially removed and depolymerized by the acidic buffer. The lipophilic extract can be removed from the biomass fiber by treatment with laccase and low-molecular-weight phenolic compounds, and LMS-activated lignin has more free radicals. Therefore, compared with control 1, the WCA of the sample prepared by control 2 is reduced to 20°. The sample obtained under the control 3 conditions has similar WCA and OCA as CP, indicating that there was little interaction between the DG and CP in the absence of laccase (Fig. 1c). However, in the presence of both laccase and DG, DGCP exhibited superlipophilicity since the OCA was 0° (Fig. 1c). The WCA of the obtained DGCP remained higher than 140°, showing that the grafting of DG onto CP was remarkably improved compared to the fibers not treated with LMS. This confirmed the role of the laccase-media system in grafting functional molecules, as laccase can graft hydrophobic compounds onto lignocellulosic surfaces. Previous studies have shown that laccase can bind DG to lignin and high-lignin content Kraft pulp (Cusola et al., 2014; Filgueira et al., 2017). This work further verified the capacity of LMS to graft DG onto complex lignocellulose, as indicated by an almost 3-fold increase in the WCA in DGCP.

To illustrate the hydrophobicity and lipophilicity of DGCP, a series of experiments was conducted. The detachment of water from DGCP is similar to the phenomenon of water droplets on a lotus leaf, which is called the "lotus effect" (Cassie Baxter state) (Tan et al., 2020). This may be mainly attributed to the high-efficiency capillary force caused by the surface of the modified material (Guan et al., 2020). As shown in Fig. 1c, the WCA of the material increased from 59.4° before modification to 140.2° after modification. Appendix A Fig. S1 shows that the contact angle of ethylene glycol was also enhanced, indicating that DGCP has a more hydrophobic surface. The dynamic contact angles of DGCP are provided in Appendix A Fig. S2, which indicates that the transient hydrophobicity of DGCP is suitable for retaining hydrophobic performance, and the WCA remains constant above 140° and only decreases by less than 1% after 240 sec. In addition, the water rolling test is shown in Appendix A movie S1. These results indicate that the hydrophobic properties of DGCP continue to be good.

The OWRK equation was utilized to calculate the surface energies of both CP and DGCP. The total surface energy of CP was 72.8 mN/m (the polar component was 35.0 mN/m and the dispersion component was 37.8 mN/m), and the total surface energy of DGCP was 43.9 N/m (the polar component was 14.3 mN/m and the dispersion component was 29.6 mN/m). Based on the data, there was a significant decrease in surface energy after LMS functionalization. Compared to that of CP, the polar component of the DGCP surface energy was reduced, indicating fewer polar groups (such as OH groups) on

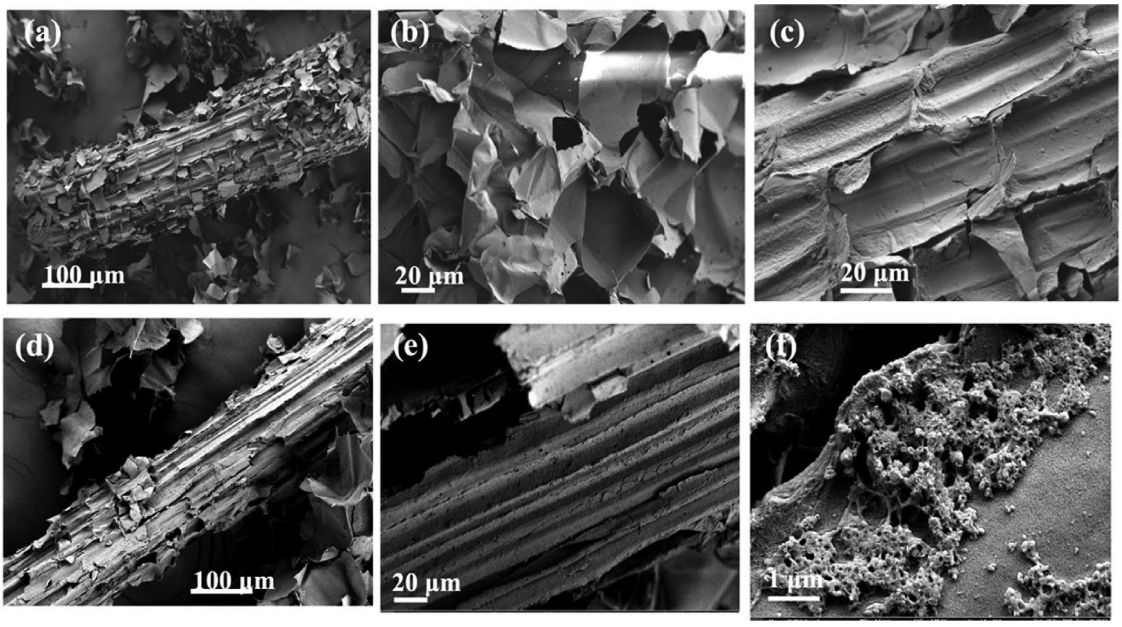

Fig. 2 – SEM images of CP before (a-c) and after (d-f) modification at different magnifications.

the surface of the material. This result may be associated with the LMS hydrolysis of the CP polymer and the grafting of hydrophobic groups from DG (Miwa et al., 2000; Yu et al., 2020). The dispersive energy value, which accounts for the van der Waals forces, declined slightly (Almasian et al., 2017). DGCP was able to maintain a hydrophobic surface toward liquids with high surface tension, such as water. Therefore, the majority of nonpolar liquids could be extensively sorbed by DGCP, while water was repelled. This property implies that DGCP can efficiently separate oily liquids from water.

2.2. *Characterization of the DGCP*

SEM images of CP and DGCP are shown in Fig. 2. CP has a clean surface as well as a honeycomb porous structure, with polygonal pores composed of thin fiber sheets with a certain depth (Fig. 2b) and with a longitudinal fiber vein (Fig. 2c). After surface modification, the fiber skeleton structure remained intact, indicating that the DGCP inherited the structural characteristics without damaging the raw material structure. Protrusions were generated on the skeleton of the DGCP (Fig. 2f).

XRD was used to detect the crystal structure of CP before and after modification. The XRD pattern is shown in Appendix A Fig. S3. The peaks of CP and DGCP are similar, but the (002) diffraction peaks showed significant broadening and exfoliation after modification. The CrI of CP is 51.17%, while that of DGCP decreased to 37.46%, indicating that the laccase broke both inter- and intramolecular hydrogen bonds in the CP, which resulted in a decrease in the degree of crystallinity (Shin et al., 2020). The structural characteristics and element composition of the sorbent play an important role in the sorption behavior of pollutants (Zhang et al., 2020). The pore structure and element composition of the material before and after modification are shown in Table S2. The BET surface areas of CP rose from 3.7999 to 5.3870 m^2/g after modification, and the pore volumes increased from 0.0048 to 0.0170 cm^3/g. The average pore diameter was also increased 3-fold. The physical properties of the obtained material prove that the DGCP produces a micro/mesoporous structure that is more conducive to the sorption of oils.

The elemental composition obtained from the elemental analysis is presented in Appendix A Table S2. DGCP was found to have an enhanced C content. This was because the LMS-mediated treatment caused long-chain compounds to graft onto the surface of the CP, leading to the modified CP having an enhanced C content compared to the raw materials. The (O+N)/C ratio was considered a sign of polarity, and O/C was considered a sign of surface hydrophilicity. Both the (O+N)/C ratio and O/C ratio of DGCP decreased, indicating that the polarity of DGCP was reduced and the hydrophilicity of the modified material was weakened. The same conclusion was drawn from the surface energy and CA analysis; that is, the polarity of DGCP was reduced, and the accessibility of water (as the polarity solution) to the surface of the material was decreased.

The chemical bonds of the materials were detected using FTIR. As shown in Fig. 3a, the wide adsorption peak at 3334 cm^{-1} is associated with hydroxyl (OH) groups (Wang et al., 2020). The band at 2918 cm^{-1} is related to the stretching of C-H. The peaks in the 1760-1680 cm^{-1} spectral region usually belong to the carbon oxygen groups of aldehydes, ketones, esters and carboxylic acids. The increased intensity of the peak at 1732 cm^{-1} may be attributed to C=O stretching from the carbon and oxygen functional groups of the grafted DG. The materials before and after modification showed a wide band in the range of 1200-900 cm^{-1}, reflecting the presence of carbon, oxygen, and hydrocarbon functional groups (Fig. 3b) (Doshi et al., 2019; Ponzini et al., 2019). The peak at 1034 cm^{-1} is due to the stretching vibration of the C-O-C bond (Zhou et al., 2018), which rises after surface functionalization,

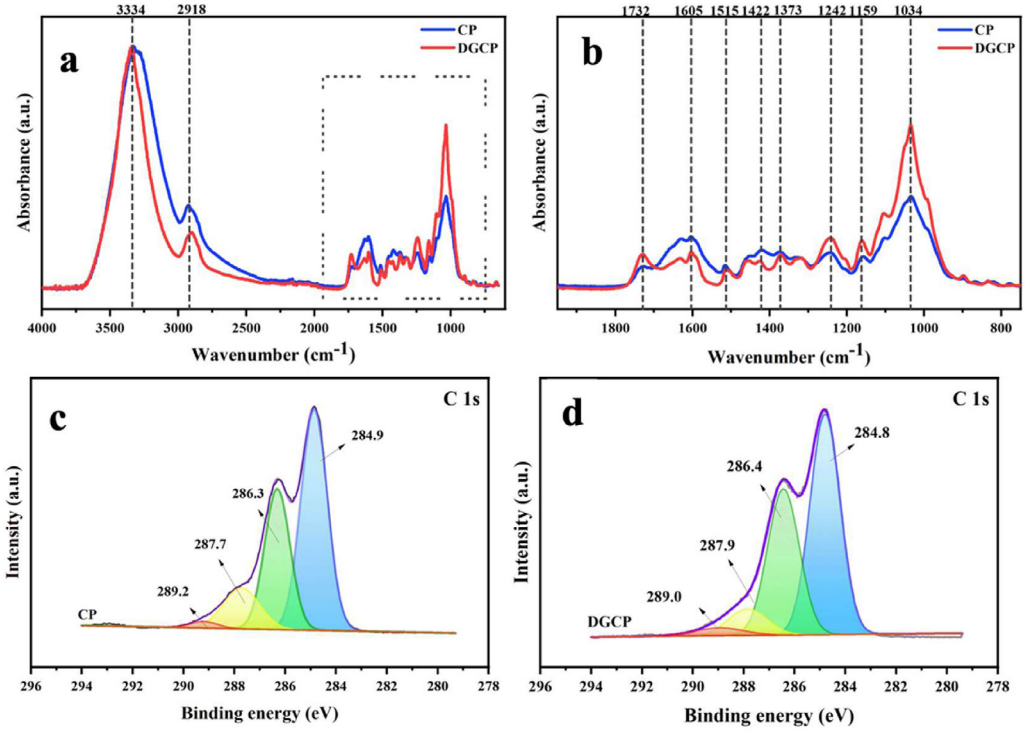

Fig. 3 – FT-IR spectra of CP and DGCP (a, b); XPS C 1s spectra of CP (c) and DGCP (d).

confirming that LMS can activate the phenolic lignin moieties to graft with DG.

X-ray photoelectron spectroscopy was used to further characterize the functional groups of the materials. As shown in Appendix A Fig. S2, both CP and DGCP contain C, N and O. Compared with the spectrum for CP, the intensity values of the C 1s and O 1s peaks in DGCP were increased, but the N 1s peak was relatively decreased. During modification, some nitrogen-containing impurities, such as proteins, may have been eluted, resulting in a decrease in the N content. To further evaluate the chemical bonds of elements, the detailed deconvolutions of the C 1s spectra for CP and DGCP were investigated (Fig. 3c, d). Through a group analysis of the C content in Appendix A Table S3, it can be found that the atomic fraction of C-O/C-OO (286.4) increased from 32.35% to 36.77%, and the change in C=O (289.0) was obvious, increasing 2-fold. The increase in the number of single-bonded groups between the carbon and oxygen confirms the coupling reaction between the oxygen free radicals in the DG and the oxygen free radicals of the CP under the treatment of the laccase-guaiacol system. This result is consistent with the peaks of the above FTIR analysis results and those of previous studies.

Hydrophobic and lipophilic materials are classic degreasing materials. They can repel water while allowing the oil phase to pass through or become easily adsorbed, thereby achieving separation of water and oil with greater efficiency and selectivity (Chen et al., 2019). Low-surface-energy chemicals can be used to adjust hydrophilic materials; thus, a long alkyl chain branch was selected in this study, as depicted in Fig. 4. For the modification of CP, the LMS treatment generated resonance-stabilized phenoxy radicals on lignin and then coupled with free radicals in DG through -O- to complete the hydrophobic long-chain alkyl connection. The surface roughness was increased, and the surface free energy was greatly reduced, which was related to the prevention of water wetting. The abundant groups of natural lignocellulosic materials make them inexpensive modified substrates to produce efficient oil sorbents.

2.3. *Sorption capacity and reusability*

To evaluate the oil sorption performance of DGCP in different liquids, water and several representative oils, such as petroleum ether, soybean oil, machine oil, and diesel, were selected. Fig. 5a shows a comprehensive comparison of the sorption capacities of untreated and modified CP. The sorption capacities of DGCP for all oils were larger than those of CP, which ranged from 38.8 to 46.43 g/g. Encouragingly, for similar oils, the sorption capacity of the modified CP was 2-3 times higher than that of raw CP, while the sorption of water was reduced by ninety-four percent. DGCP had the largest sorption capacity for machine oil, reaching 46.43 g/g, and its sorption capacity for diesel was smallest, i.e., 38.8 g/g, which is still higher than that of other reported porous straw-based sorbents, such as switchgrass (motor oil, 3.24 g/g) (Tripathi et al., 2021), candelilla wax and Fe_3O_4-coated sawdust (bean oil, 4.40 g/g) (Yin et al., 2020), C18 fatty-acid-modified cotton fiber (crude oil, 35.58 g/g) (Shin et al., 2020), lauric-acid-modified biochar (engine oil, 11 g/g) (Navarathna et al., 2020), and melamine formaldehyde lignocellulosic fibers (motor oil, 18 g/g) (Kang et al., 2020). Oil viscosity and density play key roles in the sorption capacity, and solvents with high density or low viscosity values can hardly adhere to the surfaces of sorbents, resulting in low sorption capacities. To study the effect of the

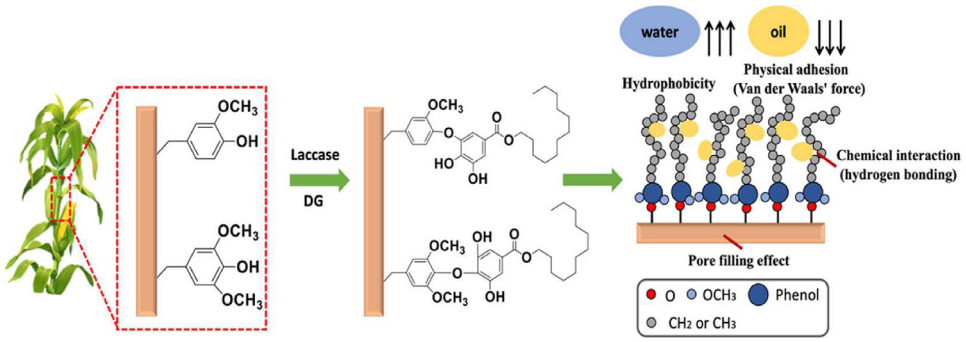

Fig. 4 – Schematic diagram showing the LMS modification of the hydrophobic grafting and interactions between different components.

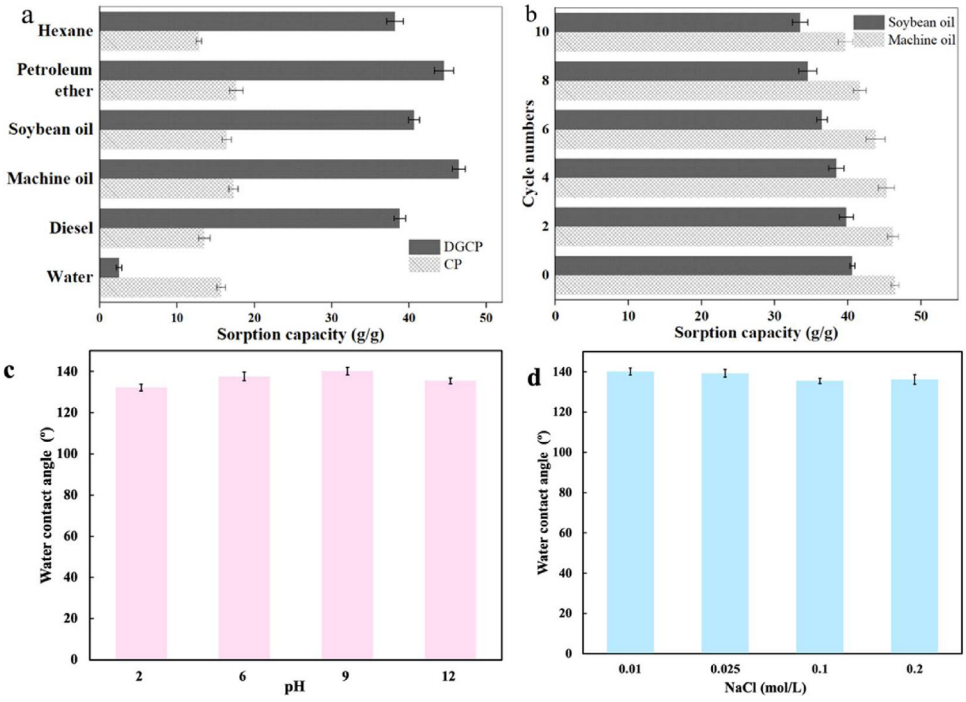

Fig. 5 – (a) Comparison of the sorption capacities of CP and DGCP for water and different oil pollutants. (b) Sorption capacities of DGCP toward machine oil and soybean oil during 10 cycles of recycling. (c) The water contact angles of DGCP after immersion in solutions of different pH values. (d) The water contact angles of DGCP after immersion in solutions of different NaCl concentrations.

initial concentration on the sorption capacity, 0.05 g of sorbent was placed in a flask containing an oil solution for 60 min at 30 °C. The experiment was repeated for various oil solution amounts (1.5, 3, 5, 7, 10, 15, 20, and 25 g) in 150 mL of freshwater. From Appendix A Fig. S4, it was observed that the best oil sorption weight of DGCP was 45.40 g/g when the initial oil amount was 20 g, and then the oil sorption capacity of the DGCP remained stable.

Reusability is an excellent characteristic for sorbents in practical applications. Therefore, the regeneration of DGCP was examined for 10 cycles of sorption-desorption with machine oil and soybean oil. After sorption, the DGCP was washed with petroleum ether and then dried in an oven for reuse. Fig. 5b shows the reusability data of the DGCP. For cycle 2, 99.4% and 98.0% of the sorption capacities toward machine oil and soybean oil, respectively, were retained. After 10 sorption–desorption cycles, the sorption capacities for both oils remained above 85%. As shown in Appendix A Fig. S5, the fiber skeleton structure of DGCP remained suitable after the recycling process. These results further highlight the potential of DGCP for decontaminating oil-polluted wastewater.

2.4. *Stability of the DGCP*

To evaluate the potential of sorbents for oil/water separation, the stability of these materials plays a key role. Numerous corrosive aqueous solutions exist during practical applications. Hence, the stability of hydrophobic materials under

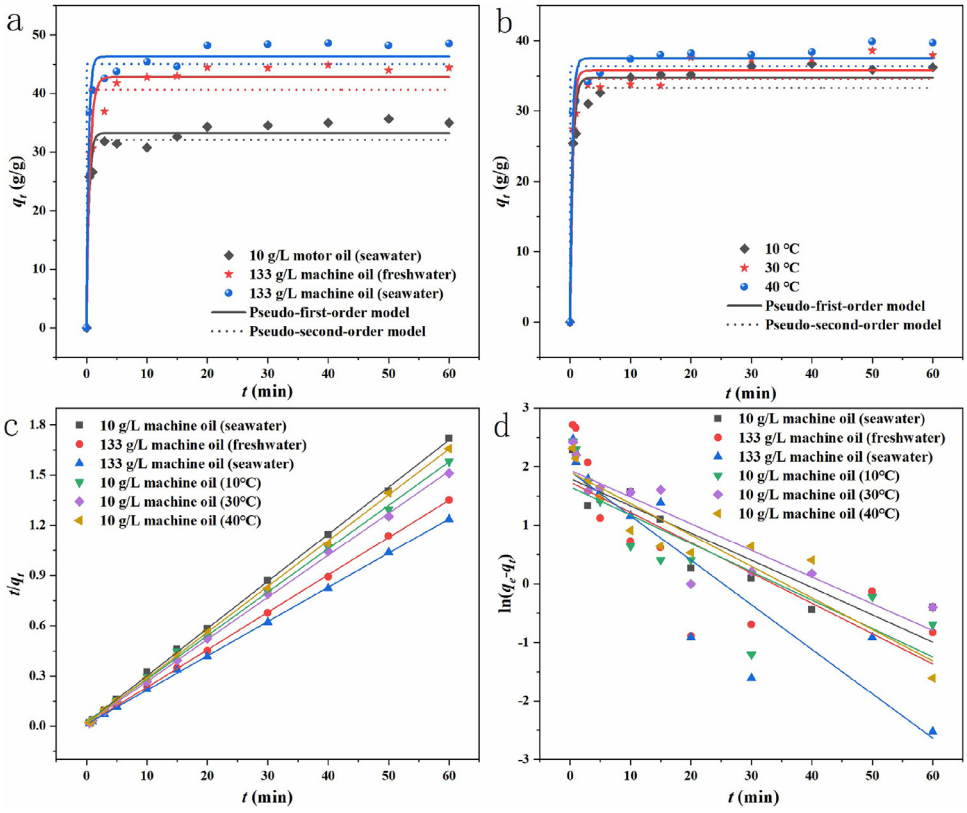

Fig. 6 – Curves of the pseudo-first-order and pseudo-second-order kinetics for DGCP ((a, b) nonlinear regression, (c, d) linear regression).

harsh conditions should be investigated. As shown in Fig. 5c, the hydrophobicity of DGCP soaked in various acid and base liquids for 6 h was not compromised. The stability at a broad pH may originate from the grafting of DG, which contains long hydrocarbon chains, onto the surface of CP, which shields the chains under harsh pH conditions. Additionally, the stability of DGCP in a series of concentrations of NaCl solution was tested. Retained hydrophobicity was observed (Fig. 5d), implying that DGCP could be used under salt conditions for oil spill recovery. These results show that DGCP has good stability and hydrophobicity. In addition, DGCP was compared with other biomass sorbents, and as shown in Appendix A Table S4, DGCP exhibited a higher sorption capacity and better reusability.

5.5. *Sorption kinetics of oil by DGCP*

Appendix A Fig. S6 shows the process of oil-water separation. The oil sorption kinetics in water at different temperatures and oil concentrations were investigated. As shown in Fig. 6a, b, the sorption capacity increases rapidly in the first 3 min, and then increases slowly. After 10 min, the sorption capacity reaches saturation. The sorption trends were similar at different oil concentrations, temperatures and aquatic media, indicating the small impact of these variables on the sorption kinetics. The sorption rate is proportional to the number of unoccupied sorption sites. In the initial stage of sorption, the number of available sorption sites is large; thus, the sorption rate is very high. As sorption proceeds, the number of unoccupied sites decreases, the sorption rate decreases and then approaches dynamic equilibrium (Zhao et al., 2020).

To better understand the sorption mechanism of oil on DGCP, pseudo-first-order, pseudo-second-order, intraparticle diffusion, and Elovich models are used to evaluate the dynamics. The adaptability of the linear and nonlinear pseudo-first-order models and the pseudo-second-order model to oil sorption are compared, and the sorption kinetic parameters obtained by the fitting process are reported in Appendix A Table S5. Through a comparison of the linear and nonlinear dynamics models, the linear form of the pseudo-second-order dynamics model has a higher correlation coefficient (R^2), indicating the applicability of the pseudo-second-order kinetic model and a better fit for the sorption process at different oil concentrations. The sorption of oil by the material at different temperatures gives the same results. The pseudo-second-order kinetics indicate that the sharing or exchange of electrons between the sorbent and oil molecules, that is, chemical sorption, may be one of the rate control steps (Wang et al., 2016). The small impact of temperature on the sorption kinetics also indicates that chemical sorption rather than physical sorption occurs (Vitela-Rodriguez and Rangel-Mendez, 2013).

Intraparticle diffusion, which is often the rate controlling step, is a possible approach for sorbate movement from the solution into the sorbent (Khezami and Capart, 2005). To determine the possible mechanisms and the effect of the rate controlling steps on the process, the data were fitted to the intraparticle diffusion model. The relationship curve between q_t

Table 1 – Isotherm parameters of DGCP.

Linear isotherm	Langmuir	Freundlich	Temkin	D-R
Parameters	q_m=46.083	K_F=3.30857	B=77.1617	q_{DR}= 43.5769
	b=0.3349	n=1.5552	b_T=922.80	E_{DR}=500
	R_L=0.8566			
R^2	0.9997	0.9708	0.9705	0.6381
SAE	218.06	3.0584	3.0749	11.245
SSE	218.06	0.0497	0.1855	0.7593
RMSE	82.418	0.0188	0.0700	0.2870
χ^2	391.98	0.0404	0.0374	0.4830
ARE	4899.9	0.5051	0.4674	6.0377
HYBRID	2331.9	0.6750	0.6245	8.1795
MPSD	73.924	1.2427	1.2011	4.4297

and $t^{1/2}$ is nonlinear over the entire time range. The curve can be divided into two parts (Appendix A Fig. S7a). The first part is linear and has a relatively high-rate constant, indicating adsorption on the outer surface. At this stage, oil molecules diffuse from the solution to the outer surface of the DGCP. However, the fitted straight line does not cross the origin, indicating that intraparticle diffusion is not the only speed-limiting step (Liu et al., 2020). The slope of the second stage is zero or almost zero, which corresponds to sorption caused by intraparticle diffusion in the pores. Since the slope is zero, it can be determined that during this period, the intraparticle diffusion process almost reaches equilibrium (the sorption between the sorbate and sorbent reaches saturation). The previous results reflect the relatively complex nature of the sorption process kinetics, in which more than one process can dominate the rate-limiting step. The Elovich model assumes that the active sites of the sorbent are heterogeneous and therefore exhibit different activation energies for chemisorption (Jiang et al., 2019). As shown in Appendix A Fig. S7b, Elovich also fits DGCP well under different environmental conditions.

2.6. *Sorption isotherms of oil by DGCP*

The sorption equilibrium data were analyzed by Langmuir, Freundlich, Temkin and Dubinin-Radushkevich (D-R) isotherms to understand how interactions occur between oils and DGCP during the sorption process (Appendix A Fig. S8). The determination carried out by using only R^2 values could not be considered a criterion for the selection of the best-fit isotherm models (Narayanan et al., 2017). To more accurately evaluate the applicability of the isotherm models in the fitting equation, several mathematical error functions were used, including the sum of absolute errors (SAE), the sum of squares (SSE), the root mean square error (RMSE), chi-square ($\chi 2$), the average relative error (ARE), the hybrid fractional error function (HYBRID) and a derivative of Marquardt's percent standard deviation (MPSD) (Ibrahim et al., 2009; Narayanan et al., 2017). Its mathematical meaning is listed in Appendix A Table S6. The parameters of the isotherm were calculated and are summarized in Table 1.

The analysis results in Table 1 show that the linear regression coefficient R^2 of the Langmuir fitting was slightly higher than that of the other models. However, for the analysis of isotherm models by other mathematical error functions, the sorption isotherm models fitted the experimental data in the following order: Temkin > Freundlich > D-R > Langmuir. As shown in Table 1, the data analysis had the best correlation with the Temkin model. The sorption b_T value of oil on DGCP was 922.80 kJ/mol, which is much higher than 80 kJ/mol, indicating its chemical nature and confirming that there is a strong interaction between oil molecules and DGCP. This phenomenon can be attributed to the similar chemical properties between the oil and the grafted long alkyl chain during the sorption process; thus, the oil wettability of DGCP was significantly improved. In addition, the b_T value was positive, which proves that the sorption process is exothermic (Miraboutalebi et al., 2017). The second-best fitting model was the Freundlich model, which reveals that the sorption of oils to the heterogeneous surfaces of DGCP followed multilayer chemisorption. The value of n was 1.5552, which showed favorable sorption since the value was between 1 and 10. Generally, it has been reported that lignocellulose-based sorbents follow the Langmuir model, which indicates that lignocellulose-based sorbents usually follow single-layer sorption (López et al., 2021) and that the sorption performance of the material is directly related to the BET surface area (Zhao et al., 2020). However, based on several error functions, the Temkin and Freundlich models offered considerably good fits with these experimental data.

2.7. *FT-IR spectra and 2D-COS maps of DGCP after oil sorption*

To further explore the sorption effects of DGCP in seawater and freshwater at different times, FT-IR was used to investigate the microstructural changes due to the interaction between oil molecules and DGCP, and the results are shown in Fig. 7a and b. In freshwater, the peak at 3350 cm^{-1} was assigned to the O-H stretching vibration in cellulose, and the bonds due to O-H stretching were increased after sorption for 20 min, indicating that the sorption of oil on DGCP was related to H-bond formation. The decrease in peaks at 2923 cm^{-1}, which was attributed to the vibration of aliphatic $–CH_2$, suggested an increase in the aromaticity groups of oil with the sorption time. The C=C stretching of the aromatic structure and C=O stretching of the carbonyl shifted from 1537 cm^{-1} to 1500 cm^{-1}, indicating that a conjugate structure formed between the oil and the aromatic structure of DGCP after sorption. In seawater (Fig. 3f), the C-OH stretching vibration in lignocellulose was observed at 3350 cm^{-1}, and the peak at 2360 cm^{-1} was attributed to C≡C or C≡N. Peaks due to the $–CH_2$ stretching vibration (1377 cm^{-1}) and aromatic C–H stretching vibration (830 cm^{-1}) were observed. The intensities of the above four vibrations were constant at different sorption times. The decreases in peaks at 2923 cm^{-1} and 1151 cm^{-1}, which were attributed to aliphatic $–CH_2$ stretching and the vibration of C-O of polysaccharides, suggested that the functional groups of DGCP were preferentially supplied during oil sorption. The peak at 1623 cm^{-1} was attributed to the asymmetric tensile vibration of COO^- in carboxylic acid, and the intensity during sorption was enhanced, which indicated that the –COOH group of DGCP may participate in the sorption interaction through hydrogen bonding. According to the

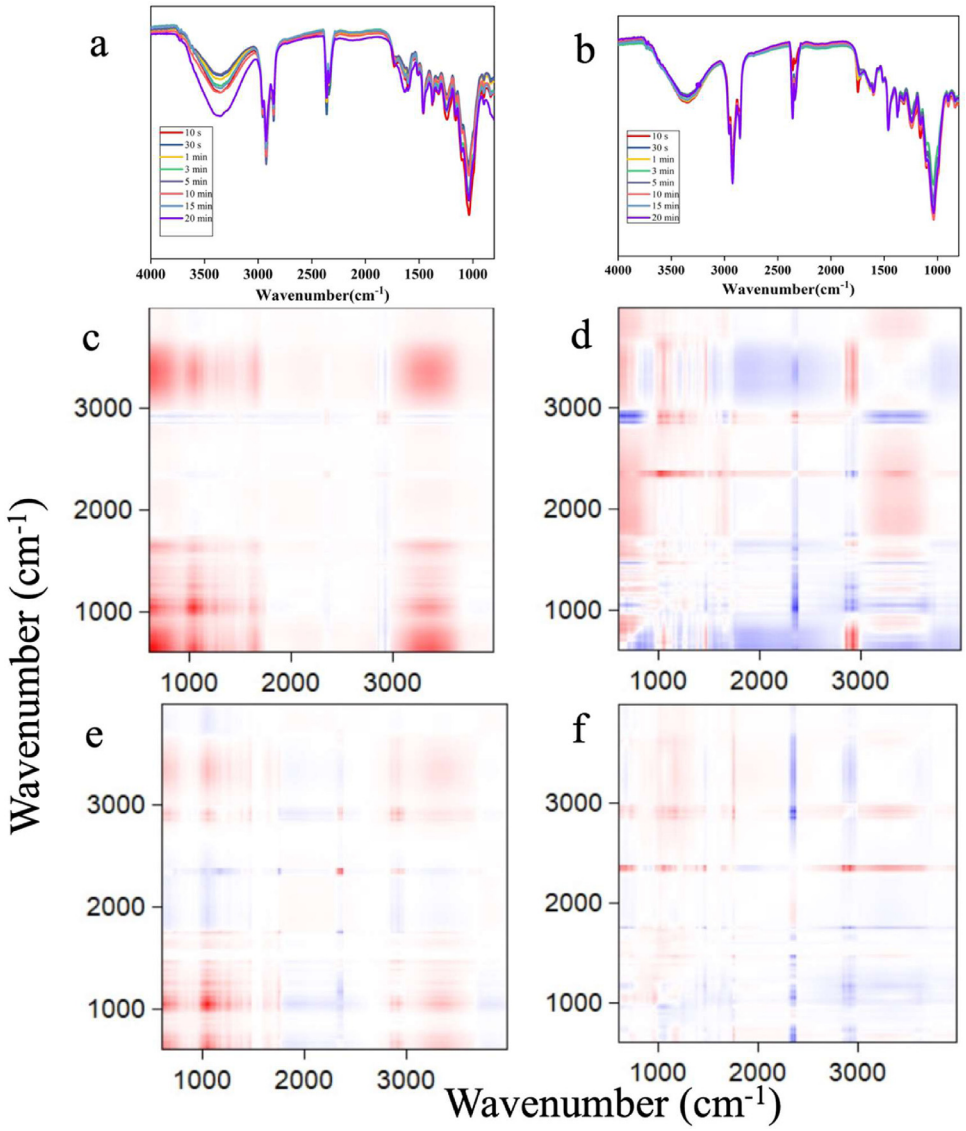

Fig. 7 – FT-IR spectra of DGCP upon oil sorption in two solutions of freshwater (a) and seawater (b) with incubation time; synchronous and asynchronous 2D-COS maps generated from FTIR spectra of DGCP upon oil sorption in two solutions, i.e., freshwater (c, e) and seawater (d, f), with incubation time.

above analysis, the sorption of oil on DGCP is dominated by chemisorption.

FT-IR spectra could provide information on chemical bonding changes but often failed to elucidate the change order of different functional bands; thus, two-dimensional correlation spectroscopy (2D-COS), based on a set of FT-IR spectra in response to external perturbations (sorption time in this study), was used to reveal the sequential changes of different functional groups. These changes are expected to illustrate the oil sorption mechanisms of DGCP during exposure to seawater and freshwater. The synchronous and asynchronous 2D FT-IR COS maps of DGCP sorbed oil in seawater and freshwater are shown in Fig. 7. In freshwater (Fig. 7c), 7 primary autopeaks were observed at 3350, 2923, 2364, 1601, 1377, 1151, and 1035 cm^{-1} in the synchronous graph. The peaks at 1035, 2923, and 3350 cm^{-1} (C-O-C stretching of polysaccharides, aliphatic $–CH_2$ stretching and O-H stretching vibration, respectively) had the highest intensity, while the peak at 1601 cm^{-1} (C=C stretching of aromatic skeletal C) had the lowest intensity. Similar to those in freshwater, 7 autopeaks were recognized (3350, 2923, 2360, 1623, 1377, 1151, and 1035 cm^{-1}) along the diagonal line in seawater (Fig. 7e), and the autopeak intensities of oil sorbed on DGCP at 1623 cm^{-1} (asymmetric tensile vibration of COO^- in carboxylic acid), 2923 cm^{-1} (vibration of aliphatic $–CH_2$) and 1151 cm^{-1} (vibration of C-O within polysaccharides) were the highest. The cross peaks in both synchronous maps of DGCP in seawater and freshwater had positive signs, suggesting that all the functional groups changed synchronously during the oil sorption process.

According to Noda's rule, the peak intensity in the synchronous spectrum can be used to reflect the influence degree of the external disturbance on functional group changes, and

the cross peak in the asynchronous correlation spectrum can be used to reflect the changing sequence of function groups with the external disturbance. In Fig. 7d and f, there were remarkable variations in the signs of the cross peaks in seawater and freshwater. For freshwater, the oil sorption process of DGCP followed the sequence 3350 (O-H stretching vibration) > 2364 (C≡C, C≡N) > 2923 (aliphatic –CH_2 stretching) > 1035 (C-O-C stretching) > 1151 (vibration of C-O within polysaccharides) > 1377 (–CH_2 stretching vibration) > 1601 (C=C). The sequential order showed that the hydroxyl groups on cellulose and oil build a strong network due to hydrogen bonds. Likewise, the sequence of characteristic peaks in seawater followed the order 1623 (C=O stretching of COOH) > 1151 (vibration of C-O within polysaccharides) > 2923 (aliphatic –CH_2 stretching) > 3350 (O-H stretching vibration) > 1377 (–CH_2 stretching vibration) > 1035 (C-O-C stretching) > 2360 (C≡C, C≡N). This result demonstrated that the asymmetric C-O stretching of free COOH groups (1623 cm^{-1}) increased, which indicated the formation of hydrogen bonds between oil and DGCP. The 2D-COS spectrum analysis revealed that hydrogen bonding between the DGCP and oil was critical in the sorption of oil, which is consistent with the results above.

3. Conclusions

CP, as an agricultural byproduct, is enzymatically modified by ecofriendly laccase with DG and is an effective sorption material for removing oil from water. Through a variety of characterization methods, the morphology and structure changes of the modified material (DGCP) are revealed. The material exhibits a rich pore structure and confirms the successful grafting of long alkyl chains, and the surface property of DGCP shows hydrophobicity with low surface energy. This oil sorbent offers good sorption capacity and reusability, i.e., the oil sorption capacity of DGCP reaches 46.43 g/g in 1 hr, and the sorption capacity remains above 85% after 10 cycles. The kinetics of the sorption process conform to the quasi-second-order kinetic model and the Elovich model, indicating a chemisorption process. The sorption process is best described by the Freundlich adsorption model, indicating the complexity of the process. The 2D FT-IR COS analysis further indicates the contribution degrees of different functional groups for oil sorption, revealing that the main mechanism of oil sorption on DGCP includes the H-bond effect, hydrophobic effect and van der Waals forces. Overall, this study developed an ecofriendly, low-cost, high-efficiency oil spill biosorbent and provided significant information for future studies on reclaiming agricultural waste.

Acknowledgments

This work was supported by the National Natural Science Foundation of China (Nos. 42007323, 42007107); the Natural Science Foundation of Guangdong Province, China(No. 2018A030313363); the Open Fund of the Guangdong Provincial Key Laboratory of Petrochemical Pollution Process and Control, China (No. 2018B030322017); the High-level Professionals and Innovative Teams, Shenzhen, China (Nos. SZIIT2019KJ024, SZIIT2019KJ007); and the Shenzhen Science & Technology Project, China (No. SZIITWDZC2021A01).

Appendix A Supplementary data

Supplementary material associated with this article can be found, in the online version, at doi:10.1016/j.jes.2021.10.019.

REFERENCES

Almasian, A., Jalali, M.L., Fard, G.C., Maleknia, L., 2017. Surfactant grafted PDA-PAN nanofiber: optimization of synthesis, characterization and oil absorption property. Chem. Eng. J. 326, 1232–1241.

Cao, X., Liu, F., Li, S., Li, L., 2008. Study on optimization production process of porous starch with high capacity of adsorption for oil. J. Sichuan Univer. Sci. Eng. (Nat. Sci. Ed.) 21 (1), 60–65.

Chen, C., Weng, D., Mahmood, A., Chen, S., Wang, J., 2019. Separation mechanism and construction of surfaces with special wettability for oil/water separation. ACS Appl. Mater. Interfaces 11, 11006–11027.

Cusola, O., Valls, C., Vidal, T., Roncero, M.B., 2014. Rapid functionalisation of cellulose-based materials using a mixture containing laccase activated lauryl gallate and sulfonated lignin. Holzforschung 68 (6), 631–639.

Doshi, B., Hietala, S., Sirviö, J.A., Repo, E., Sillanpää, M., 2019. A powdered orange peel combined carboxymethyl chitosan and its acylated derivative for the emulsification of marine diesel and 2T-oil with different qualities of water. J. Mol. Liq. 291, 111327 -111327.

Filgueira, D., Holmen, S., Melbø, J.K., Moldes, D., Echtermeyer, A.T., Chinga-Carrasco, G., 2017. Enzymatic-assisted modification of thermomechanical pulp fibers to improve the interfacial adhesion with poly(lactic acid) for 3D printing. ACS Sustain. Chem. Eng. 5, 9338–9346.

Guan, X., Jiang, H., Ngai, T., 2020. Pickering high internal phase emulsions templated super-hydrophobic–oleophilic elastic foams for highly efficient oil/water separation. ACS Appl. Poly. Mater. 2, 5664–5673.

Ibrahim, S., Ang, H.M., Wang, S., 2009. Removal of emulsified food and mineral oils from wastewater using surfactant modified barley straw. Bioresour. Technol. 100, 5744–5749.

Jiang, C., Wang, X., Qin, D., Da, W., Hou, B., Hao, C., et al., 2019. Construction of magnetic lignin-based adsorbent and its adsorption properties for dyes. J. Hazard. Mater. 369, 50–61.

Kang, L., Wang, B., Zeng, J., Cheng, Z., Li, J., Xu, J., et al., 2020. Degradable dual superlyophobic lignocellulosic fibers for high-efficiency oil/water separation. Green Chem. 22, 504–512.

Khezami, L., Capart, R., 2005. Removal of chromium(VI) from aqueous solution by activated carbons: kinetic and equilibrium studies. J. Hazard. Mater. 123, 223–231.

Lan, Z., Dan, P., Chu-ling, G., Chao-fei, Z., Xiu-ling, X., Zhi, D., 2013. Preparation and performance investigation of trichoderma viride-modified corn stalk as sorbent materials for oil spills. Environ. Sci. 34, 1605–1610.

Liu, G., Liao, L., Dai, Z., Qi, Q., Wu, J., Ma, L.Q., et al., 2020. Organic adsorbents modified with citric acid and Fe_3O_4 enhance the removal of Cd and Pb in contaminated solutions. Chem. Eng. J. 395, 125108.

López, Y.C., Ortega, G.A., Martínez, M.A., Reguera, E., 2021. Magnetic Prussian blue derivative like absorbent cages for an efficient thallium removal. J. Clean Prod. 283 (10), 124587.

Luo, Y.Q., Song, X., Song, F., Wang, X.L., Wang, Y.Z., 2019. A fully bio-based composite coating with mechanical robustness and

dual superlyophobicity for efficient two-way oil/water separation. J. Colloid Interface Sci. 549, 123–132.
Miraboutalebi, S.M., Nikouzad, S.K., Peydayesh, M., Allahgholi, N., Vafajoo, L., McKay, G., 2017. Methylene blue adsorption via maize silk powder: Kinetic, equilibrium, thermodynamic studies and residual error analysis. Process. Saf. Environ. 106, 191–202.
Miwa, M., Nakajima, A., Fujishima, A., Hashimoto, K., Watanabe, T., 2000. Effects of the surface roughness on sliding angles of water droplets on superhydrophobic surfaces. Langmuir 16, 5754–5760.
Mogharabi, M., Faramarzi, M.A., 2014. Laccase and Laccase-mediated systems in the synthesis of organic compounds. Adv. Synth. Catal. 356, 897–927.
Narayanan, N., Gupta, S., Gajbhiye, V.T., Manjaiah, K.M., 2017. Optimization of isotherm models for pesticide sorption on biopolymer-nanoclay composite by error analysis. Chemosphere 173, 502–511.
Navarathna, C.M., Bombuwala Dewage, N., Keeton, C., Pennisson, J., Henderson, R., Lashley, B., et al., 2020. Biochar adsorbents with enhanced hydrophobicity for oil spill removal. ACS Appl. Mater. Interfaces 12, 9248–9260.
Ni, S., Liu, N., Fu, Y., Gao, H., Qin, M., 2021. Laccase mediated phenol/chitosan treatment to improve the hydrophobicity of Kraft pulp. Cellulose 28, 4397–4409.
Oliveira, L., Saleem, J., Bazargan, A., Duarte, J., McKay, G., Meili, L., 2021. Sorption as a rapidly response for oil spill accidents: a material and mechanistic approach. J. Hazard. Mater. 407, 124842.
Owens, D.K., Went, R.C., 1969. Estimation of the surface free energy of polymers. J. Appl. Polym. Sci. 13, 1741–1747.
Ponzini, E., Natalello, A., Usai, F., Bechmann, M., Peri, F., Muller, N., et al., 2019. Structural characterization of aerogels derived from enzymatically oxidized galactomannans of fenugreek, sesbania and guar gums. Carbohydr. Polym. 207, 510–520.
Shin, Y., Han, K.S., Arey, B.W., Bonheyo, G.T., 2020. Cotton fiber-based sorbents for treating crude oil spills. ACS Omega 5, 13894–13901.
Tan, X., Wang, H-M.D., Zang, D., Wu, L., Liu, F., Cao, G., et al., 2020. Superhydrophobic/superoleophilic corn straw as an eco-friendly oil sorbent for the removal of spilled oil. Clean Technol. Environ. 23, 145–152.
Tripathi, J., Arya, A., Ciolkosz, D., 2021. Switchgrass as oil and water-spill sorbent: Effect of particle size, torrefaction, and regeneration methods. J. Environ. Manag. 281, 111908.
Vitela-Rodriguez, A.V., Rangel-Mendez, J.R., 2013. Arsenic removal by modified activated carbons with iron hydro(oxide) nanoparticles. J Environ. Manag. 114, 225–231.
Wang, H., Xu, X., Ren, Z., Gao, B., 2016. Removal of phosphate and chromium(VI) from liquids by an amine-crosslinked nano-Fe_3O_4 biosorbent derived from corn straw. RSC Adv. 6, 47237–47248.
Wang, Z., Saleem, J., Barford, J.P., McKay, G., 2020. Preparation and characterization of modified rice husks by biological delignification and acetylation for oil spill cleanup. Environ. Technol. 41, 1980–1991.
Xue, J., Cheng, D., Li, N., Xiao, X., Bai, Y., Gao, Y., et al., 2021. Durable hydrophobic Enteromorpha design for controlling oil spills in marine environment prepared by organosilane modification for efficient oil-water separation. J. Hazard. Mater. 421, 126824.
Yin, Z., Li, Y., Song, T., Bao, M., Li, Y., Lu, J., et al., 2020. Preparation of superhydrophobic magnetic sawdust for effective oil/water separation. J. Clean Prod. 253, 120058.
Yu, T., Halouane, F., Mathias, D., Barras, A., Wang, Z., Lv, A., et al., 2020. Preparation of magnetic, superhydrophobic/superoleophilic polyurethane sponge: Separation of oil/water mixture and demulsification. Chem. Eng. J. 384, 123339.
Zhao, J., Yu, L., Ma, H., Zhou, F., Yang, K., Wu, G., 2020. Corn stalk-based activated carbon synthesized by a novel activation method for high-performance adsorption of hexavalent chromium in aqueous solutions. J. Colloid Interface Sci. 578, 650–659.
Zhang, Y., Yin, M., Lin, X., Ren, X., Huang, T-S., Kim, I.S., 2019. Functional nanocomposite aerogels based on nanocrystalline cellulose for selective oil/water separation and antibacterial applications. Chem. Eng. J. 371, 306–313.
Zhang, Y., Zhang, Y., Cao, Q., Wang, C., Yang, C., Li, Y., et al., 2020. Novel porous oil-water separation material with super-hydrophobicity and super-oleophilicity prepared from beeswax, lignin, and cotton. Sci. Total. Environ. 706, 135807.
Zhou, G., Ma, Y., Fan, T., Wang, G., 2018. Preparation and characteristics of a multifunctional dust suppressant with agglomeration and wettability performance used in coal mine. Chem. Eng. Res. Design 132, 729–742.
Zhou, Q., Wu, W., Zhou, S., Xing, T., Sun, G., Chen, G., 2020. Polydopamine-induced growth of mineralized γ-FeOOH nanorods for construction of silk fabric with excellent superhydrophobicity, flame retardancy and UV resistance. Chem. Eng. J. 382, 122988.
Zhu, H., Huang, Y., Xia, F., 2020. Environmentally friendly superhydrophobic osmanthus flowers for oil spill cleanup. Appl. Mater. Today 19, 100607.
Zimmerman, J.B., Anastas, P.T., Erythropel, H.C., Leitner, W., 2020. Designing for a green chemistry future. Science 367, 397–400.